Supporting Information

Barium disilicide as a promising thin-film photovoltaic absorber: structural, electronic, and defect properties

Mukesh Kumar*,#,§ Naoto Umezawa*,#,§, Wei Zhou, #,ξ and Motoharu Imai‡

International Center for Materials Nanoarchitectonics (MANA), National Institute for Materials Science, 1-1 Namiki, Tsukuba, Ibaraki 305-0044, Japan

ς School of Physics and Materials Science, Thapar University, Patiala-147004, India

§ CREST, Japan Science and Technology Agency, 4-1-8 Honcho, Kawaguchi, Saitama, 332-0012, Japan

ξ Department of Applied Physics, Institute of Advanced Materials Physics, Tianjin Key Laboratory of Low Dimensional Materials Physics and Preparing Technology, School of Science, Tianjin University, Tianjin 300072, People's Republic of China

‡ Research Center for Functional Materials, National Institute for Materials Science, Ibaraki 305-0047, Japan

***Corresponding author**
Email: mkgarg79@gmail.com
Email: Umezawa.Naoto@gmail.com

1. Born-effective charges

The Born-effective charges Z* is a fundamental quantity that manifest the strength of the charge transfer with respect to the displacement of atom. It is also a useful tool to investigate the degree of covalency and ionicity in particular bonding to some extent. The calculated sum of the Born effective charges fulfil the acoustic sum rule $\sum_s Z^*_{s,ij} = 0$.

In a conventional unit cell of $BaSi_2$, eight Ba occupy two inequivalent 4*c* Wyckoff sites. We designated these as B(I) with fractional coordinate x = 0.017, y=0.25, z = 0.692) and B(II) with x = 0.839, y=0.25, z = 0.092. Similarly, 16 Si occupy three inequivalent positions at 4*c* and 8*d* Wyckoff sites, we designated these as Si(I) with x = 0.416, y=0.25, z = 0.091), Si(II) with x = 0.198, y=0.25, z = 0.966), and Si(III) with x = 0.195, y=0.734, z = 0.145 fractional coordinates. In this case, the sum rule is as follows: Z*[Ba(I)]+ Z*[Ba(II)]+ Z*[Si(I)]+ Z*[Si(II)]+2 Z*[Si(III)] = 0.

The formal static charge of Ba and Si in $BaSi_2$ compound are +2 and -1 respectively. We can see from table S1 that all these compounds have large Z* compared with their nominal static charges.

This large variation in Z* compared to nominal static charge confirms the charge transfer in $BaSi_2$ system also show the covalent bonding character of Si atoms.

Table S1 Calculated Born effective charge (Z^*) of Ba_2Si_4. Here we presented Z^*_{XX}, Z^*_{YY}, Z^*_{ZZ} and Z^*_{avg} for two inequivalent sites Ba(I), B(II) of Ba atom and three inequivalent sites, Si(I), Si(II) and Si(III) of Si atoms.

	Born effective charges Z* (*e*)				
	Ba(I)	Ba(II)	Si(I)	Si(II)	Si(III)
Z^*_{XX}	2.42	2.95	-1.18	-1.98	-1.10
Z^*_{YY}	3.33	2.30	-1.22	-1.28	-1.58
Z^*_{ZZ}	3.07	2.42	-0.94	-2.11	-1.23
Z^*_{avg}	2.94	2.56	-1.11	-1.79	-1.30

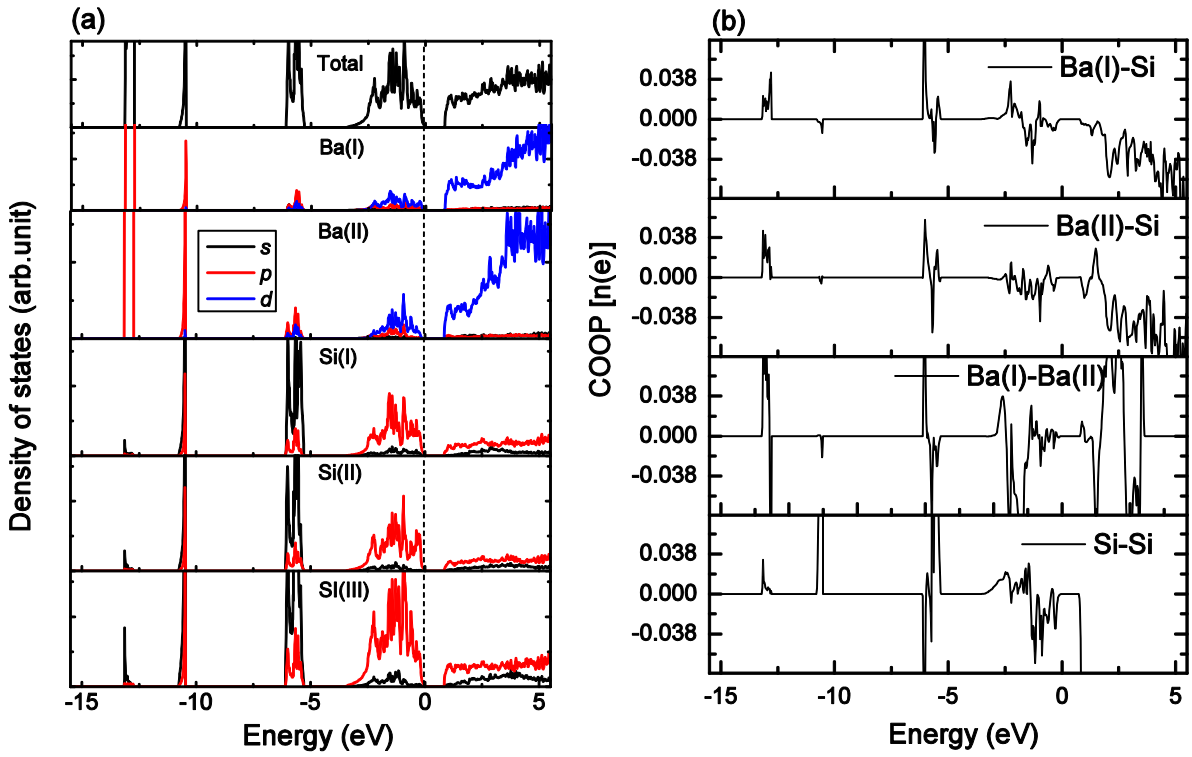

Figure S1 Calculated (a) total and orbital decomposed density of states, (b) crystal population for the different bonds in $BaSi_2$.

Table S2 Calculated fundamental band gap (E_g) and other various energy gaps of BaSi2 at various high symmetry points of BZ in the unit eV, together with the available experimental data.

	PBE	HSE06	GW0	Exp.
E_g	0.77	1.25	1.28	1.1–1.3[a]
E_g^{dir}	0.86	1.37	1.38	
E_g^{Γ}	1.22	1.68	1.75	
E_g^{X}	1.79	2.32	2.38	
E_g^{Y}	0.97	1.48	1.48	
E_g^{Z}	1.50	2.01	2.10	
E_g^{T}	1.05	1.55	1.58	

[a] T. Suemasu, Jpn. J. Appl. Phys. 54 (7S2), 07JA01 (2015).

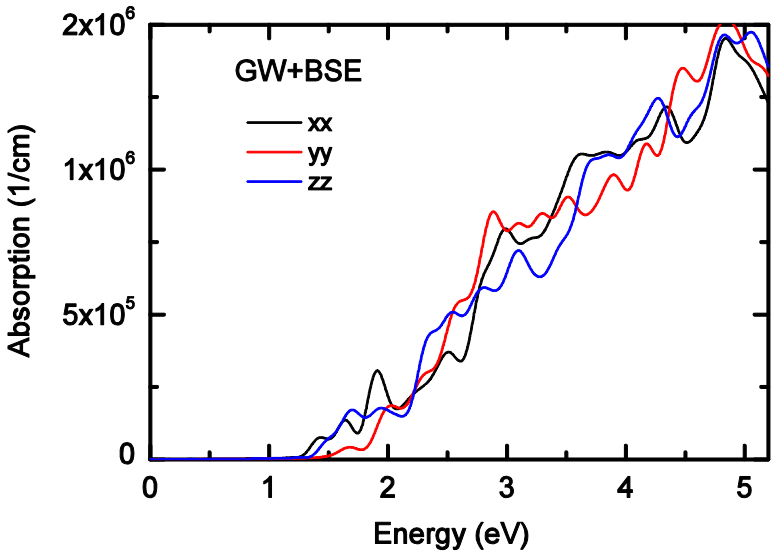

Figure S2 GW+BSE absorption coefficient $\alpha(\omega)$ of $BaSi_2$ in all three crystallographic directions xx (black line), yy (red line) and zz (blue line). One can see that there is considerable absorptions along all the directions.

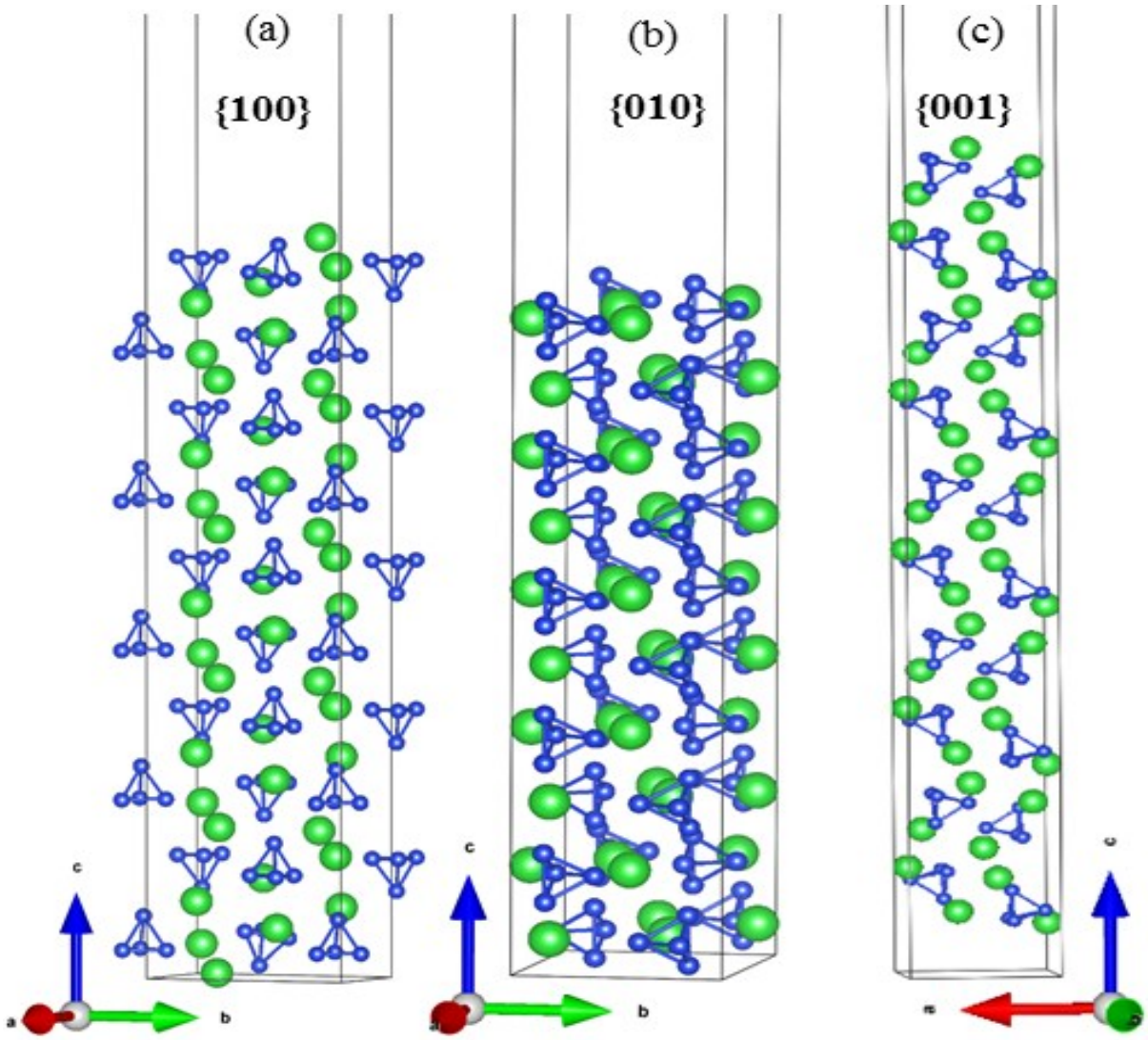

Figure S3 Relaxed geometries for the (a) (100), (b) (010) and (c) (001) surfaces of $BaSi_2$ based on a 120-atom slab model. Here, big green balls represent Ba atom, while small blue balls represent Si atom.

4. Defect studies

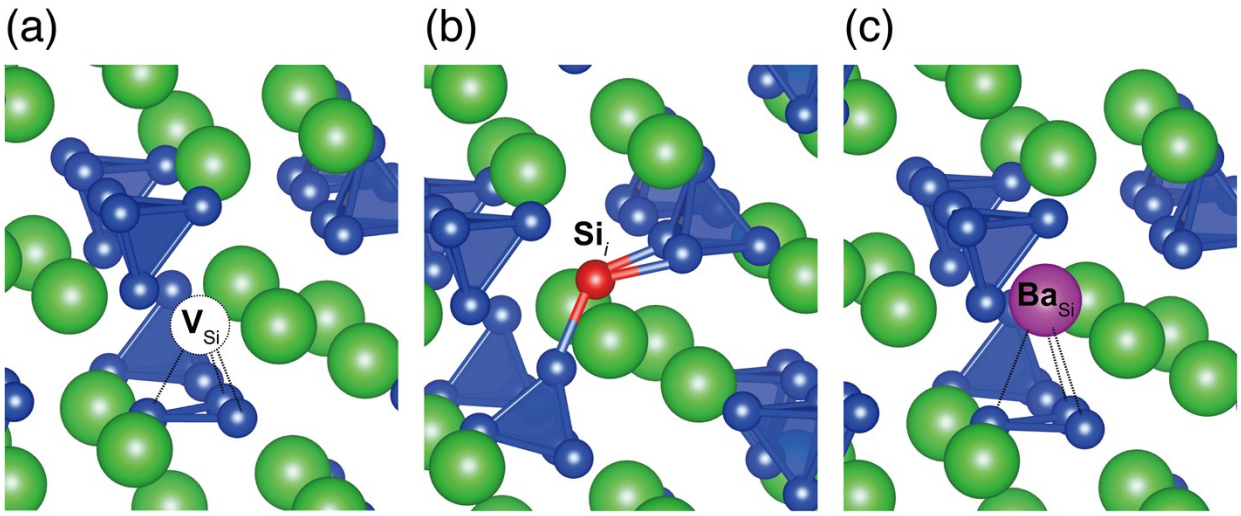

Figure S4 Local geometries of relaxed structures for (a) singly positive silicon vacancy (V_{Si}^{+}), (b) silicon interstitial (Si_i^0), and (c) barium substituted for silicon (Ba_{Si}^0). The relaxed Si_i^0 is off the plane coordinated with three nearest neighbour silicon atoms, while an in-plane site was suggested by the previous work [*J Appl Phys* **2014**, 116 (12), 12370928], which was adopted for an initial configuration of Si_i^0 in the present study.

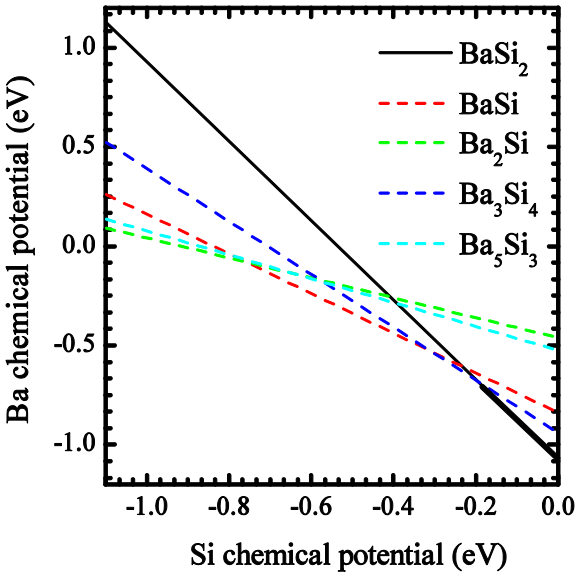

Figure S5 Thermodynamic stable chemical potential domain for $BaSi_2$.

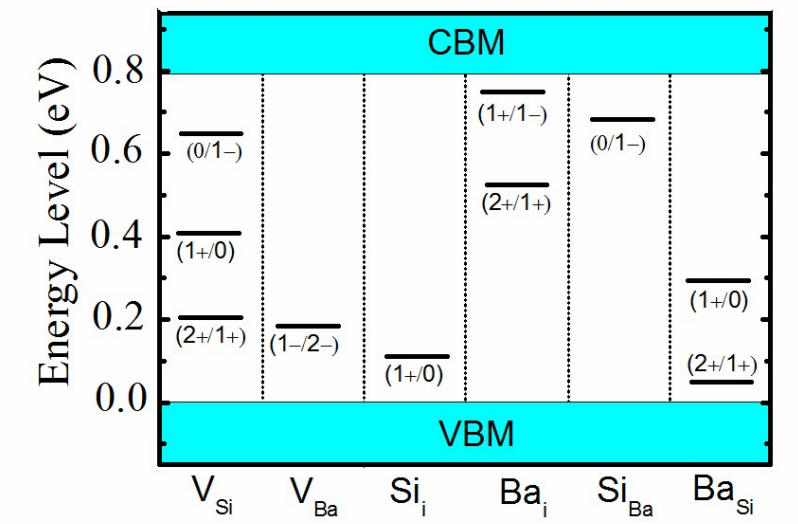

Figure S6 The ionization levels of intrinsic defects in the DFT band gap (~0.8 eV) of $BaSi_2$. The initial and final charge states are labeled in parentheses.

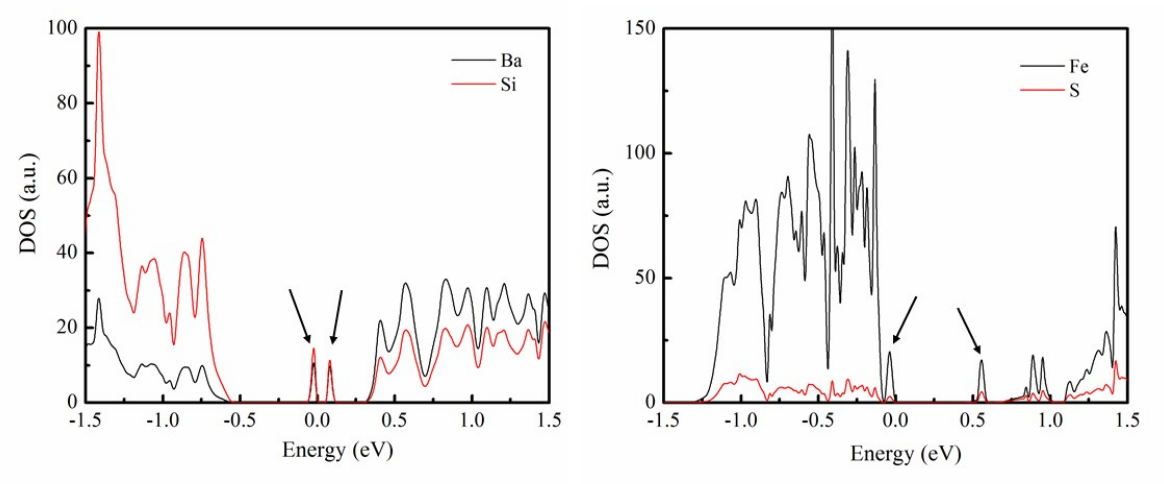

Figure S7 Density of states near band edges for anion vacancy in (a) $BaSi_2$ and (b) FeS_2 compounds. Black arrows indicate the defcet levels.

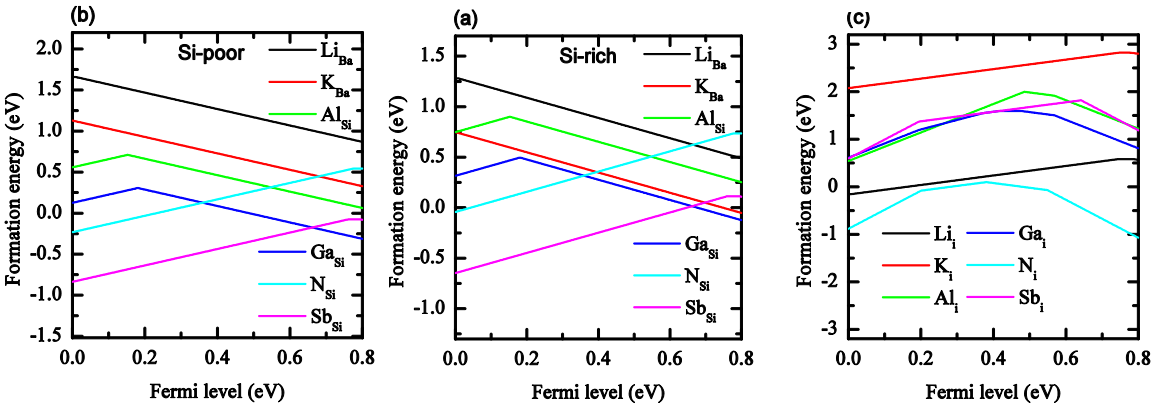

Figure S8 Calculated formation energies as a function of the Fermi energy (DFT band gap) for (a) and (b) substitutional and (c) interstitial dopants (Si-rich condition) in $BaSi_2$.

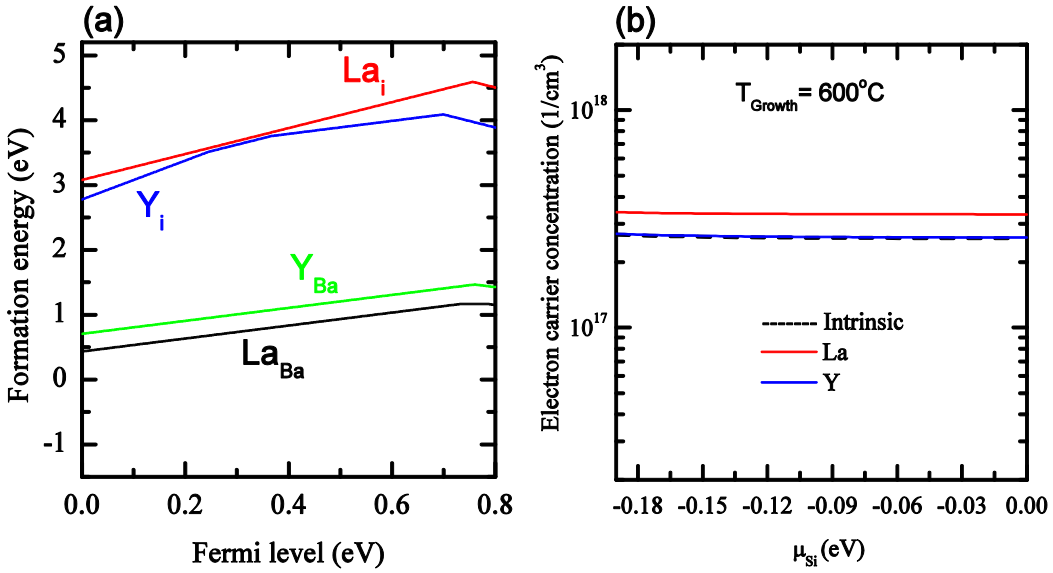

Figure S9 Calculated (a) defect formation energy and (b) electron carrier density with La and Y doping in $BaSi_2$.

Table S3 Calculated DFT chemical potential of various external dopants.

Element	Structure	Chemical potential (eV/atom)
Li	Cubic	-1.902
K	Cubic	-1.047
Al	Cubic	-3.740
Ga	Orthorhombic	-2.909
N_2	Gas	-8.295
Sb	Trigonal	-4.142

Table S4 Doping concentrations for considered external dopants.

Dopants		Defect concentration (cm^{-3})	
		Si_rich	Si_poor
donors	Li_i^{+1}	$1.3x10^{19}$	$1.1x10^{19}$
	N_i^{+1}	$2.3x10^{18}$	$1.9x10^{18}$
	Sb_{Si}^{+1}	$3.4x10^{21}$	$1.6x10^{22}$
	La_{Ba}^{+1}	$1.3x10^{17}$	$1.2x10^{17}$
	Y_{Ba}^{+1}	$4.3x10^{15}$	$4.3x10^{15}$
acceptors	K_{Ba}^{-1}	$5.4x10^{18}$	$3.9x10^{17}$
	Al_{Si}^{-1}	$9.9x10^{17}$	$4.3x10^{18}$
	Ga_{Si}^{-1}	$3.3x10^{19}$	$3.8x10^{20}$